16TH EUROPEAN CONFERENCE ON EARTHQUAKE ENGINEERING THESSALONIKI 18 - 21 JUNE 2018

FRACTAL AND COMPLEXITY ANALYSIS OF CRACK PATTERNS OF MASONRY WALLS

Amir REZAIE[1], Antoine J.P. MAURON[2], Kiarash M. DOLATSHAHI[3], Katrin BEYER[4]

ABSTRACT

In order to develop automatic image-based methods for damage evaluation after earthquakes, crack maps need to be evaluated using computer-based algorithms. A common method to link the crack map to a damage state is to compute the fractal dimension of the crack map by the box-counting method. In this paper, it is shown that determining the fractal dimension by the box-counting method can lead in some cases to erroneous interpretations of the level of the damage as an increase in the number of cracks does not necessarily lead to an increase in the fractal dimension. To tackle this issue, the fractal dimension is computed by another method, the extended box counting method. It is observed that this estimation of the fractal dimension can better capture the increase in the number of cracks. The method is applied to masonry walls and it is shown that a good correlation between the complexity dimension and the stiffness loss ratio exists.

Keywords: Masonry; Crack pattern; Fractal dimension; Complexity; Box-counting method; Extended box-counting method.

1. INTRODUCTION

Damage assessment of structural elements using non-destructive methods has received significant attention. With the advent of cameras that are able to take high-resolution photos and unmanned aerial vehicles (UAVs), image-based methods can be developed that combine automatic damage detection techniques on images with methods that analyze the crack patterns quantitatively (ATC, 1998; Grünthal, 1998; Galarreta, Kerle and Gerke, 2015) These quantitative measures can then be linked to a change in structural properties, such as stiffness loss. The latter can then be used to update finite element models and reevaluate the seismic safety of the structure.

Rather than considering physical properties of crack maps like length, width, direction and location, the fractal characteristics of the pattern on an image, such as the fractal dimension (Lopes and Betrouni, 2009), lacunarity (Plotnick, Gardner and O'Neill, 1993) or the succolarity (de Melo and Conci, 2013), can be used to evaluate the damage state and to predict the properties of the damaged structural elements. The most common way of characterizing crack maps by fractal dimensions is to analyze the crack map by means of the box-counting method. While the characterization of crack patterns by fractal dimensions has been investigated, it is not yet very widely used in civil engineering applications. In structural engineering, Sun et al. (2011) explored the relation between the applied load and the fractal dimension of cracks on the surface of concrete beams. They found that the size of aggregate has an effect on the

[1]Doctoral assistant, Earthquake Engineering and Structural Dynamics Laboratory (EESD), School of Architecture, Civil and Environmental Engineering (ENAC), École Polytechnique Fédérale de Lausanne (EPFL), EPFL ENAC IIC EESD, GC B2 515, Station 18, CH – 1015 Lausanne, Switzerland, amir.rezaie@epfl.ch

[2] Graduate student, Earthquake Engineering and Structural Dynamics Laboratory (EESD), School of Architecture, Civil and Environmental Engineering (ENAC), École Polytechnique Fédérale de Lausanne (EPFL), EPFL ENAC IIC EESD, GC B2 515, Station 18, CH – 1015 Lausanne, Switzerland, antoine.mauron@epfl.ch

[3]Assistant professor, Department of Civil Engineering, Sharif University of Technology, Tehran, Iran, dolatshahi@sharif.edu

[4]Associate professor, Earthquake Engineering and Structural Dynamics Laboratory (EESD), School of Architecture, Civil and Environmental Engineering (ENAC), École Polytechnique Fédérale de Lausanne (EPFL), EPFL ENAC IIC EESD, GC B2 515, Station 18, CH – 1015 Lausanne, Switzerland, katrin.beyer@epfl.ch

crack growth. Issa et al. (2003) explored the relationship between the toughness of the fracture surface of concrete specimens and the fractal dimension of the crack pattern. They concluded that by increasing the toughness of the fracture area, the fractal dimension of the crack pattern increases. Using monofractal and multifractal analysis of crack patterns on reinforced concrete structures, Maosen et al. (Cao, Ren and Qiao, 2006) showed that there is an approximately linear relationship between fractal quantities and some traditional damage indicators like natural frequency and average carbonized depth. Yang et al. (Yang, He and Dai, 2017) used fractal dimensions of crack patterns to characterise the damage of the reinforced concrete beams at the failure stage.

Recently, researchers have investigated the crack patterns of reinforced concrete walls (Farhidzadeh *et al.*, 2013; Ebrahimkhanlou, Farhidzadeh and Salamone, 2016; Carrillo and Avila, 2017; Carrillo, Dominguez and Prado, 2017). They established correlations between the fractal and multifractal dimensions of the crack maps and the overall structural properties such as stiffness loss and maximum attained drift ratios. Farhidzadeh et al. (Farhidzadeh *et al.*, 2013) proposed a formula to relate the value of the damage index (DI) based on fractal dimension to the relative stiffness loss ratio of large-scale rectangular concrete shear walls. They observed a good agreement between the results of the fractal damage index and the relative stiffness loss ratio obtained from the experimental test. Ebrahimkhanlou et al. (Ebrahimkhanlou, Farhidzadeh and Salamone, 2016) evaluated the reinforced concrete shear walls by multifractal analysis of the crack patterns. They showed that different crack growth, both at small and large scales, could be addressed by the multifractal analysis, which is useful when assessing automatically the state of concrete walls. Carrillo and Avila (Carrillo and Avila, 2017) put forward some empirical relations between fractal dimension and the maximum attained story-drift ratio of thin and lightly reinforced concrete walls that can serve for estimating the current performance of the cracked walls. For brick masonry walls, Dolatshahi and Beyer (Dolatshahi and Beyer, 2018) proposed another expression based on both textural and structural fractal dimensions to estimate the stiffness loss ratio and strength degradation. They observed satisfactory agreement between the suggested formula and the experimental results.

It is evident that using fractal characteristics of the crack patterns to evaluate the damage of a structure, is less time-consuming, less subjective compared to the visual inspection and opens up new possibilities with regard to automated inspection methods. However, in this paper we show that there are also some drawbacks of estimating the fractal dimensions by the standard box-counting method, which has been used in previous structural engineering applications, and that other methods, namely the extended box-counting method might be a suitable alternative method. . The paper commences by introducing the standard box-counting method and discussing some limitations of the method for analyzing the fractal characteristics of a crack pattern. Thereafter, another way of evaluating the fractal dimension of an object that is referred to as “extended box-counting method” is explained. The advantages of using the latter method over the box-counting method is then discussed. Finally, some correlations between the so-obtained complexity dimensions and stiffness loss ratios of masonry walls, which were tested at EPFL (Petry and Beyer, 2015), are established. The results indicate that the relationship between the stiffness loss ratio and the complexity dimension in a specific magnification range follows a linear trend that could in the future be used in post-earthquake assessment situations for estimating the residual stiffness and strength of damaged elements once it has been validated for a large set of unreinforced masonry walls.

2. FRACTAL AND COMPLEXITY ANALYSIS

Fractal dimensions, mainly developed by Mandelbrot (Mandelbrot, 1983), are used to determine the irregularity, complexity and space filling properties of an object (Mandelbrot, 1983; Corbit and Garbary, 1995; Sandau, 1996; Di Ieva *et al.*, 2007). One of the properties of a mathematical fractal set is self-similarity over the infinite range of scales; however, natural fractals are statistically self-similar only over a specific range of scales (Buczkowski *et al.*, 1998; Falconer, 2004).

In practical cases, there are a number of methods to compute the fractal dimension of an object, among which the box-counting method (BCM) is one of the most widely used approaches (Falconer, 2004; Lopes and Betrouni, 2009; Farhidzadeh *et al.*, 2013; Ebrahimkhanlou, Farhidzadeh and Salamone, 2016; Carrillo and Avila, 2017; Carrillo, Dominguez and Prado, 2017). The estimated fractal dimension using

the BCM depends on various parameters that need to be chosen when applying the BCM. These include the minimum and maximum box size (Ostwald, 2013), the scale factor (Ostwald, 2013; So, So and Jin, 2017) and the grid position (Bouda, Caplan and Saiers, 2016; Di Ieva, 2016).
Sandau (Sandau, 1996) proposed another method that is called the extended box-counting method (XBCM). It computes the fractal dimension over a specific range of magnification. Sandau and Kurz (1997) stated that for arbitrary structures, a dimension representing the complexity, which they called the "x-dim", should be investigated rather than fractal dimensions that are estimated by BCM. In this method, the dimension is calculated based on the most complex region of the set (Sandau, 1996). Better preservation of the union stability—the dimension of the union of two arbitrary sets must be equal to the maximum dimension of the two individual sets—makes this method superior to the BCM. Comparing two images, Sandau and Kurz (1997) showed that in some cases, although the visual complexity of one of the images was higher than the other, the fractal dimension computed by the BCM was lower for the complex pattern. The main reason for this contradictory results is the use of the least-squares method in the BCM to obtain the best fitted line, which slope determines the fractal dimension (Sandau, 1996).
In this study it is shown that in particular cases, the value of the box-counting dimension decreases as the cracks grow and fill more regions of the wall—the crack pattern becomes more complex. In the following sections, the BCM and the XBCM are introduced and advantages of using XBCM rather than BCM are investigated.

2.1 Box-Counting Method

To estimate the fractal dimension of a pattern by BCM, a set of grids with various box sizes r is placed on the object and the number $N(r)$ of the boxes intersecting the pattern, here the crack map, is counted. The value of the fractal dimension FD is determined as (Falconer, 2004; Lopes and Betrouni, 2009):

$$FD = -\lim_{r \to 0} \frac{\log N(r)}{\log r} \tag{1}$$

In practice, $\log N(r)$ versus $\log r$ is plotted and then the slope of the graph over the range of scales where points fall on a straight line is determined by the method of least squares (Peitgen, Jürgens and Saupe, 2006). The absolute value of the slope is the box-counting dimension that is the estimation of fractal dimension (FD^{BCM}). This method is not only applied to fractal geometries but also to patterns that are not exactly self-similar (Peitgen, Jürgens and Saupe, 2006; Feldman, 2012; Di Ieva, 2016), such as crack maps. As an illustration, two crack maps of the same wall are shown in Figure 1—the wall has the dimension 2000 mm x 2000 mm and the scale of the image is 1 pixel=1 mm. The stair-stepped cracks of the second pattern cover a larger region than the stair-stepped crack of the first pattern. The FD^{BCM}s of these two patterns are calculated as follows:

1) First, the smallest rectangle covering the crack map is determined, namely the "bounding box" (Karperien, 2007)— in Figure 1 the bounding box is depicted with red color;
2) The boxes are squares and have the sizes of 2^n pixels, where n=1,2,3,…m (Peitgen, Jürgens and Saupe, 2006);
3) The lower limit is set to 2 pixels and the upper limit of the interval is supposed to be less than half of the minimum size of the bounding box, i.e., the upper limit is 2^m with $m = \max\{n | 2^n < \min(\text{bounding box})/2\}$ (Foroutan-pour, Dutilleul and Smith, 1999; Roy *et al.*, 2007; Harrar and Hamami, 2009);
4) The origin of the grid corresponds to the bottom left corner of the bounding box;
5) The horizontal and vertical lines of the lattice are assumed to be parallel to the horizontal and vertical edges of the image, respectively (Bouda, Caplan and Saiers, 2016).

It can be seen that there is a linear correlation between $\log N(r)$ and $\log r$ in the considered magnification range with a high value of coefficient of determination, which means that the pattern can be described by reporting just one dimension. In some cases, there could be an apparent slope change

that shows the fact that the object has different dimensions in various range of scales (Peitgen, Jürgens and Saupe, 2006) and two line must be fitted to the points. The FD^{BCM}s for the crack map I and II are 1.01 and 1.00, respectively, though the visual complexity of the crack map II is higher than the visual complexity of the crack map I. Thus, if the box-counting algorithm is used as an automated method to evaluate the level of damages, according to the computed FD^{BCM}s, one can infer that in the second stage the wall has experienced a slightly lower level of damage, which is not correct. Indeed, the main reason for such a misleading result stems from the methodological issues tied to the BCM, including the influence of the box sizes, the positions of the grids and the least square procedure (Buczkowski *et al.*, 1998; Foroutan-pour, Dutilleul and Smith, 1999; Roy *et al.*, 2007; Ostwald, 2013; So, So and Jin, 2017). The results show that the FD^{BCM}s for the two crack maps are almost the same and equal to one meaning that horizontal, vertical, diagonal and stair step cracks lead to the same fractal dimension estimated by this method. From a physical point of view, however, they have diverse effects on the overall and local response of the wall. It is worthwhile noting that the box-counting dimension is always around one when few disconnected cracks are dispersed over the structure. Since in this case, the boxes only intersect the lines at small scales; therefore, the estimated fractal dimension tends toward the topological dimension of a line that is one. The following section seeks to define another measure for the fractal dimension of the crack pattern, aiming at discriminating between the two crack maps with various levels of complexity.

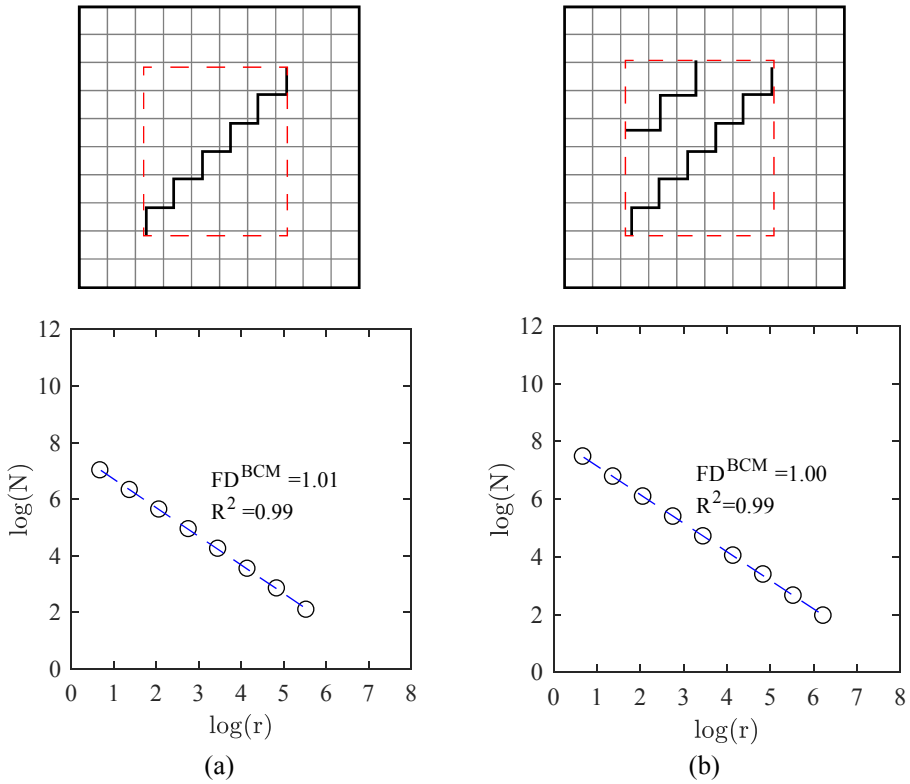

Figure 1. Crack maps and the corresponding FD^{BCM}
a) crack map I b) crack map II

2.2 Extended Box-Counting Method

The extended box-counting method can be used to calculate the fractal or complexity dimension of a set that has been termed x-dimension (Sandau, 1996) that in this paper, is referred to as FD^{XBCM}:

a) A set of masks with various grid sizes is considered as schematically shown in Figure 2. In this figure, the grid size is a and the mask size is b. Pragmatically speaking, it is advised to use powers of 2 (i.e. 2,4,8,…) for both a and b (Sandau, 1996). The minimum size of the grid (a) is recommended to be at least two pixels and the maximum size of the mask (b) is restricted by the minimum size of the image (Sandau, 1996). In this paper, to compute FD^{XBCM}s for the crack patterns of the tested walls, the mask sizes are moved over the image by a step size that is lower

than the minimum size of the brick (200 mm), to reduce the computational cost.

b) Then, the image is scanned by a given mask and the number N of the small boxes, which comprise at least one black pixel, is counted. Figure 3 pinpoints a typical crack map in masonry walls that is covered by a mask.

c) The position of the mask must change through the whole image to find the mask with the maximum number of N, i.e. $N = N_{max}$.

d) The fractal dimension or complexity dimension is obtained based on the mask size b and grid size a as follows:

$$FD^{XBCM} = \frac{\log_2 N_{max}}{\log_2 b - \log_2 a} \tag{2}$$

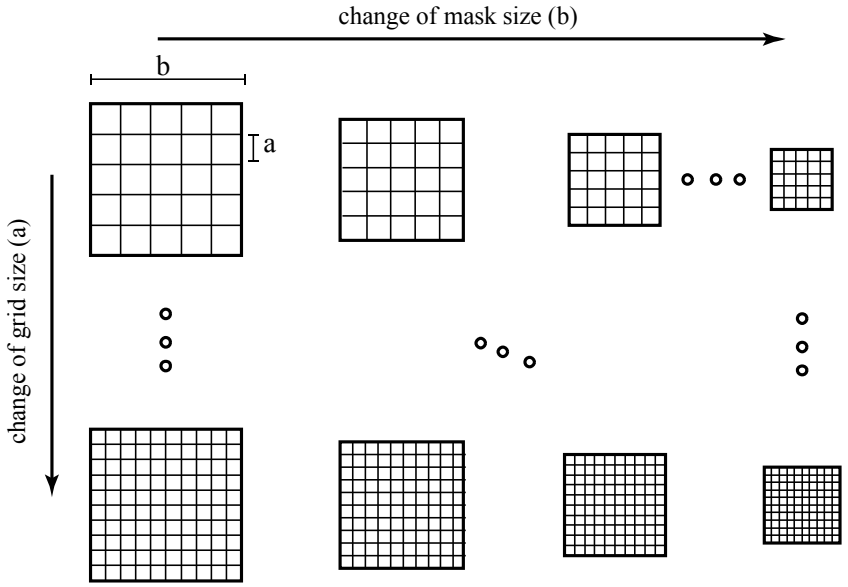

Figure 2. Illustration of mask and grid sizes

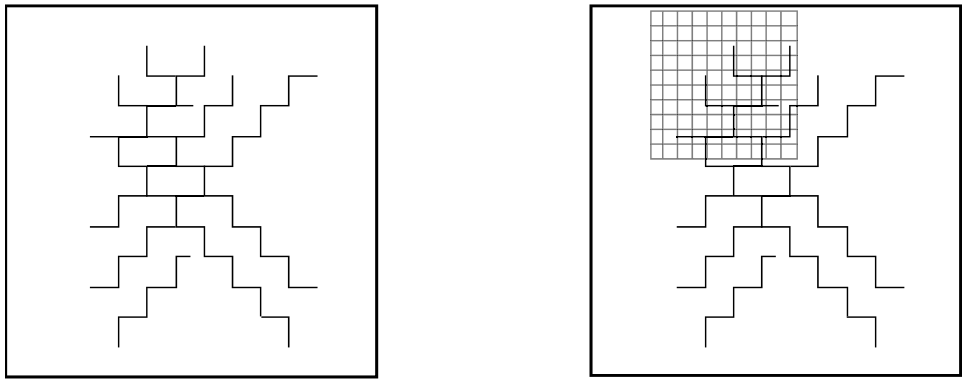

Figure 3. Covering of an image by a given mask
a) crack map b) covering by a mask

Now the values of FD^{XBCM} for the crack maps illustrated in Figure 1 are computed in order to make a comparison between the results of XBCM and BCM. Figure 4 shows that the complexity dimension FD^{XBCM} of the crack map II is higher than the crack map I, which corresponds to the visual complexities of these patterns. The other advantage of XBCM is that different FD^{XBCM}s can be obtained according to the given mask and grid sizes, which allows exploring the complexity of the crack patterns in various scale ranges. Here, a wide range for a and b are used to investigate the complexity of the pattern at different scales. It can be inferred that utilizing FD^{XBCM} to investigate the damage assessment of structural elements in a specific period is advantageous over the conventional box-counting dimension,

for as the crack grows and covers the element, the value of the complexity dimension also increases. In the following section, the application of FD^{XBCM} for the damage assessment of masonry walls under quasi-static load is addressed.

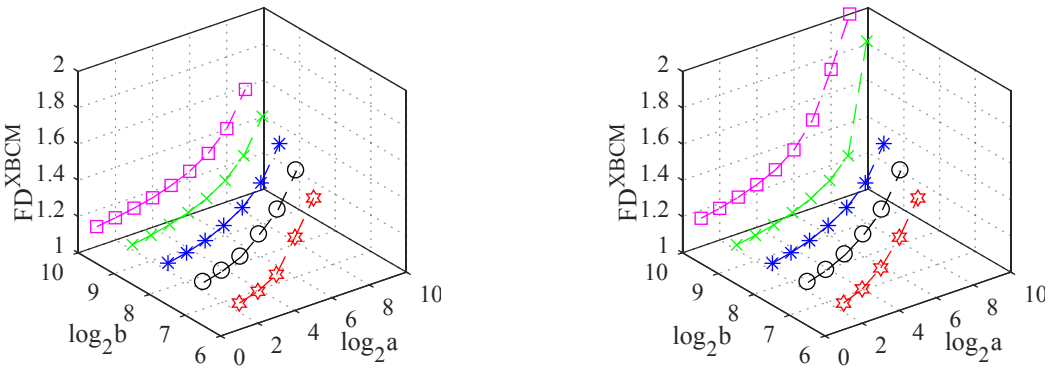

(a) Crack map I (b) Crack map II

Figure 4. Fractal dimensions computed by XBCM

2.3 Case study

In this section, the complexity dimensions of the crack maps of the brick masonry walls with a length of 2010 mm and height of 2250 mm, namely PUP, tested under quasi-static conditions at EPFL (Petry and Beyer, 2015) are computed. To prepare the images for applying the extended box-counting method, the skeletonized binary crack patterns at each drift ratio are drawn in AutoCAD (2011) with the scale ratio of 1 pixel/mm. As an illustration, Figure 5 and Figure 6 show the crack maps and corresponding complexity dimensions at various drift limits for wall PUP2, respectively.

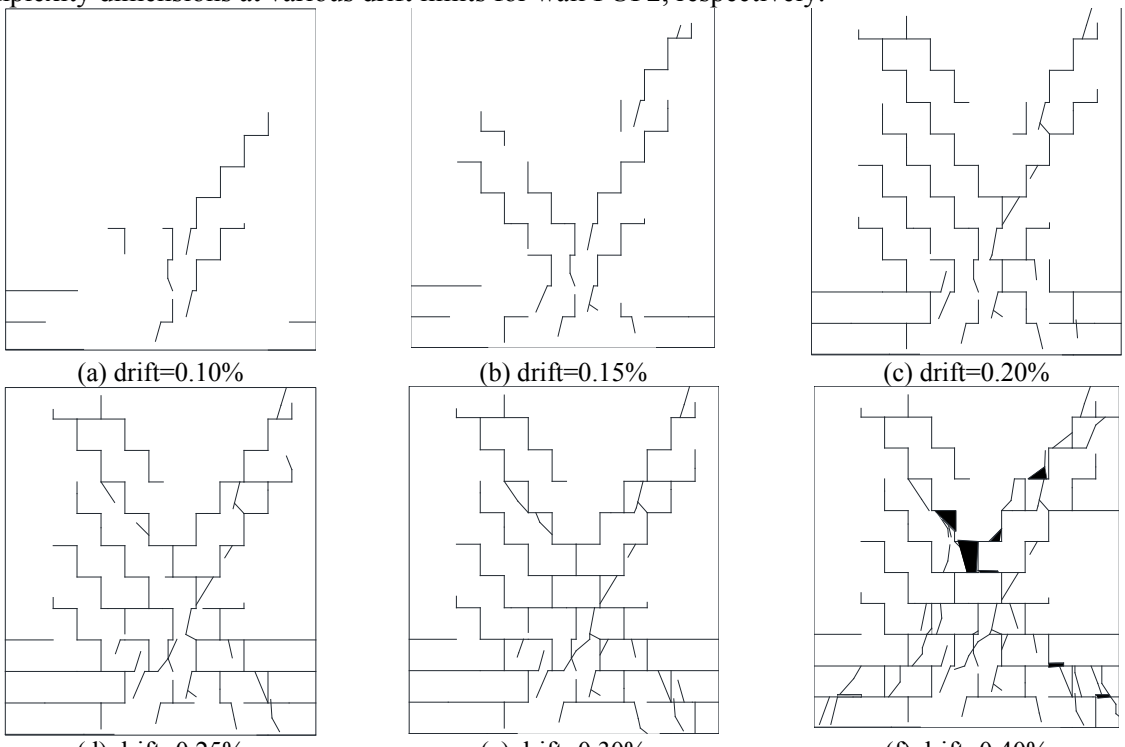

(a) drift=0.10% (b) drift=0.15% (c) drift=0.20%

(d) drift=0.25% (e) drift=0.30% (f) drift=0.40%

Figure 5. Crack maps of the tested wall PUP2

It can be observed that in general, the value of the FD^{XBCM} increases as the cracks grow with increasing drift ratios. This is due to the fact that FD^{XBCM} values are computed based on the position of the mask where the number of intersected boxes is maximum. Moreover, for a given mask size, by increasing the

size of the grid, the obtained FD^{XBCM} becomes higher, although the number of intersected boxes declines. This rise continues until there is a mask position where all the grid boxes include at least one black pixel that leads to the FD^{XBCM} of two, which implies that the crack pattern almost covers the whole area in the given magnification range.

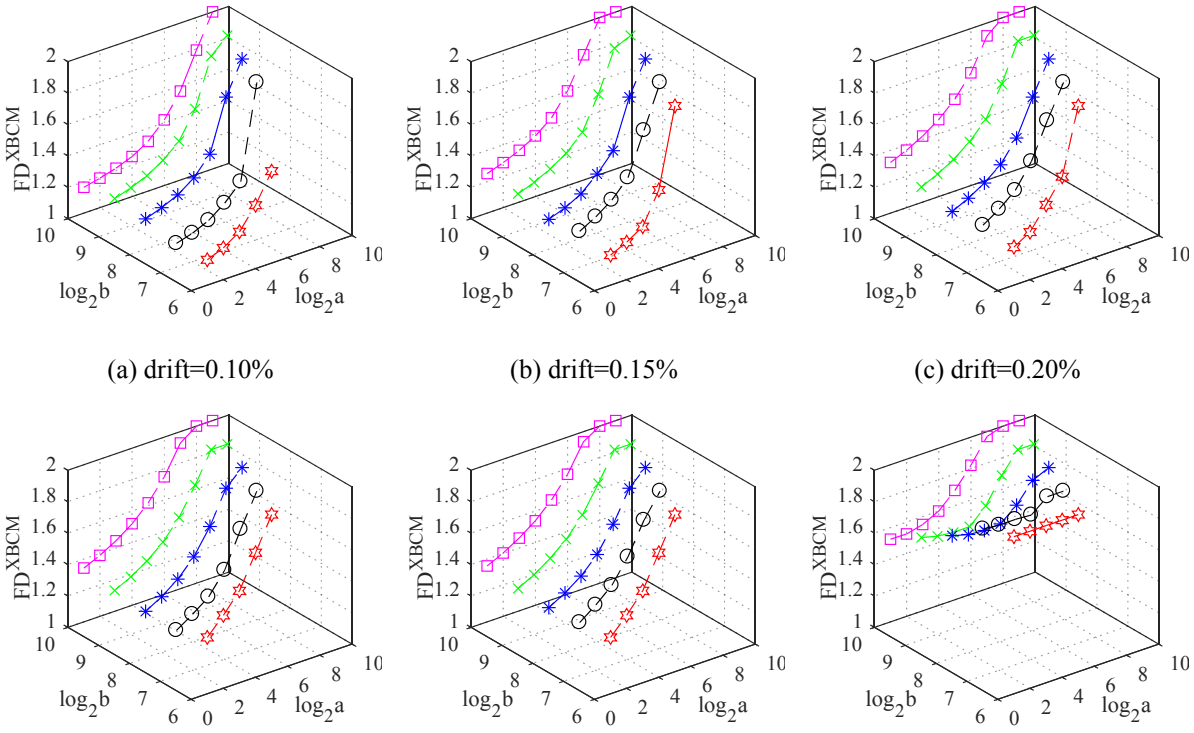

(a) drift=0.10% (b) drift=0.15% (c) drift=0.20%

(d) drift=0.25% (e) drift=0.30% (f) drift=0.40%

Figure 6. Complexity results (wall PUP2)

Now, the efficiency of the box-counting and extended box-counting methods in estimating stiffness degradation of the walls (PUP2-6) during the test is compared. To do so, the stiffness loss ratio predicted by BCM and XBCM is obtained according to Equation 3 and Equation 4, respectively:

$$SL_P^B = FD^{BCM} - 1 \quad (3)$$

$$SL_P^X = FD^{XBCM} - 1 \quad (4)$$

where SL_P denotes the predicted secant stiffness loss ratio. Moreover, the secant stiffness loss ratio of the tested wall SL_T is defined as:

$$SL_T = 1 - \frac{K_j}{K_i} \quad (5)$$

in which K_i stands for initial stiffness of the wall and K_j is the secant stiffness of the wall at the maximum drift ratio of each cycle.

For computing the box-counting dimensions FD^{BCM}, the range over which the pattern shows fractal behavior is used to fit the straight line. Here the linear line is fitted for dimensions between the height of the brick and half the minimum size of the bounding box. For calculating the complexity dimensions FD^{XBCM}, the size of the mask is considered 1024 mm based on the suggestion in Sandau (1996), which is roughly equal to half the minimum wall dimension. However, the size of the grid is assumed variable to evaluate which size correlates best with the stiffness loss.

In Figure 7, the comparison between the stiffness loss ratios obtained in the experiment and those predicted by the standard box-counting algorithm is shown. In the ideal case, the data must fall on the red line, meaning the error in estimating the stiffness loss ratio by fractal analysis is zero. It can be seen that the coefficient of determination is rather small and the data are largely scattered with respect to the red line.

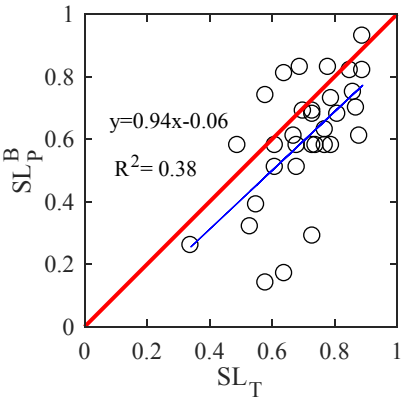

Figure 7. Graph of stiffness loss ratio obtained in the test and predicted by BCM

According to Figure 8, it can be seen that there is a linear correlation between the stiffness loss ratios obtained in the experiment and the one predicted by the XBCM. Furthermore, in comparison with Figure 7, the data are better correlated and the coefficients of determination for all considered grid sizes are higher. Considering a grid size of 64 mm results in the best estimate of the stiffness loss as the data are closest to the ideal red line. For other grid sizes where there is a deviation from the red line, applying a constant to the computed fitted line can reduce the error of prediction. In both grid sizes, 16 and 32 mm, the stiffness loss ratios are underestimated whereas considering 128 mm results in conservative stiffness loss ratio prediction. It is worth mentioning that generally as the grid size increases, so does the contribution of every single crack pixel to the rise of the complexity dimension.

In theory, it is observed that using the XBCM for defining a correlation between the stiffness loss ratio and fractal dimensions of the crack maps is superior over the standard BCM. However, it is necessary to choose a suitable grid size or to apply a constant coefficient to the obtained fitted line to predict the stiffness loss ratios.

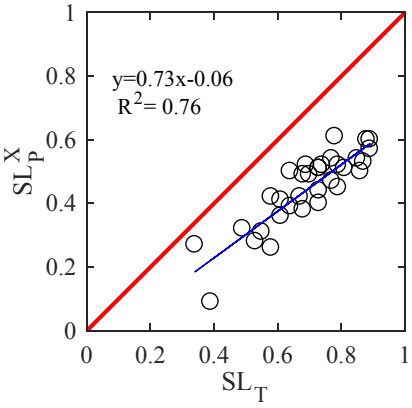

(a) grid size=16 mm

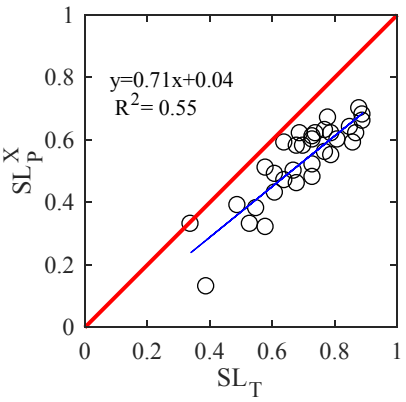

(b) grid size=32 mm

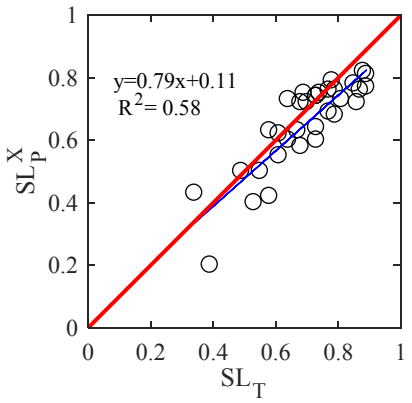

(c) grid size=64 mm

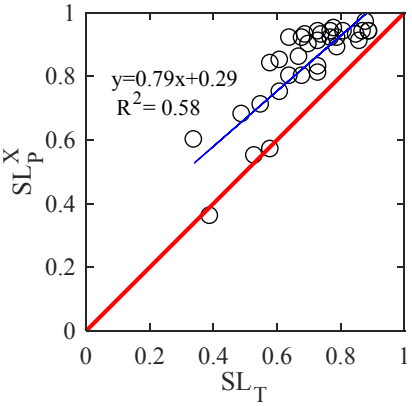

(d) grid size=128 mm

Figure 8. Graph of stiffness loss ratio obtained in the test and predicted by XBCM

3. CONCLUSIONS

In structural engineering applications, fractal dimensions of crack patterns have so far been estimated by applying the classical box-counting method (FD^{BCM}). The resulting estimates of the fractal dimensions of the crack pattern were used to define correlations between the damage to the structural element and physical properties of the structure such as the loss of stiffness. In this paper, it was shown that due to some shortcomings of the classical box counting method, it might be better to use another dimension, namely the x-dimension or complexity dimension (FD^{XBCM}), which is capable of representing visual complexity based on the concept of fractals. To be more specific, it was observed that in some cases, although the space-filling characteristic of the crack pattern increases along with the visual complexity, the box-counting dimension FD^{BCM} decreases. On the other hand, because the complexity dimension FD^{XBCM} depends on the most complex part of the image, its trend is always increasing as the complexity of the crack pattern rises. To verify the capability of the extended box counting method for estimating the stiffness loss of damaged unreinforced masonry walls, the relationship between the stiffness loss ratio of walls tested at EPFL and the complexity dimensions of the crack maps was determined. It was found that FD^{XBCM} correlates well with the stiffness loss ratio of the masonry walls. As a result, the complexity dimension FD^{XBCM} could be used as a quantitative measure to explore the current condition of the masonry walls. Future work will aim at generalizing the relationships between FD^{XBCM} and stiffness loss relationships for a large range of wall dimensions as well as static and kinematic boundary conditions.

4. REFERENCES

ATC (1998) *FEMA-306: Evaluation of earthquake damaged concrete and masonry wall buildings. Basic Procedures Manual*. Washington, D.C.: Applied Technology Council (ATC).

Autodesk (2011) 'AutoCAD Civil 3D, student version, Copyright © 2012 Autodesk, Inc. http://students.autodesk.com/'.

Bouda, M., Caplan, J. S. and Saiers, J. E. (2016) 'Box-Counting Dimension Revisited: Presenting an Efficient Method of Minimizing Quantization Error and an Assessment of the Self-Similarity of Structural Root Systems', *Frontiers in Plant Science*. Frontiers Media S.A., 7, p. 149. doi: 10.3389/fpls.2016.00149.

Buczkowski, S., Kyriacos, S., Nekka, F. and Cartilier, Lo. (1998) 'The modified box-counting method: Analysis of some characteristic parameters', *Pattern Recognition*, 31(4), pp. 411–418. doi: https://doi.org/10.1016/S0031-3203(97)00054-X.

Cao, M., Ren, Q. and Qiao, P. (2006) 'Nondestructive assessment of reinforced concrete structures based on fractal damage characteristic factors', *Journal of Engineering Mechanics*, 132(9), pp. 924–931. doi: 10.1061/(ASCE)0733-9399(2006)132:9(924).

Carrillo, J. and Avila, W. (2017) 'Assessment of seismic damage of thin and lightly reinforced concrete walls using fractal dimension of cracking', *Earthquake Engineering & Structural Dynamics*, 46(4), pp. 661–675. doi: 10.1002/eqe.2808.

Carrillo, J., Dominguez, D. and Prado, N. (2017) 'Seismic Damage Index Based on Fractal Dimension of Cracking on Thin Reinforced Concrete Walls', *ACI Structural Journal*. American Concrete Institute, 114(6), pp. 1649–1658.

Corbit, J. D. and Garbary, D. J. (1995) 'Fractal Dimension as a Quantitative Measure of Complexity in Plant Development', *Proceedings: Biological Sciences*. Royal Society, 262(1363), pp. 1–6.

Dolatshahi, K. M. and Beyer, K. (2018) 'Estimation of the loss of stiffness and strength of damaged unreinforced brick masonry walls using fractal analysis', *Submitted to Journal of Earthquake Engineering*.

Ebrahimkhanlou, A., Farhidzadeh, A. and Salamone, S. (2016) 'Multifractal analysis of crack patterns in reinforced concrete shear walls', *Structural Health Monitoring*. SAGE Publications, 15(1), pp. 81–92. doi:

10.1177/1475921715624502.

Falconer, K. (2004) *Fractal geometry: mathematical foundations and applications*. Chichester: John Wiley & Sons.

Farhidzadeh, A., Dehghan-Niri, E., Moustafa, A., Salamone, S. and Whittaker, A. (2013) 'Damage Assessment of Reinforced Concrete Structures Using Fractal Analysis of Residual Crack Patterns', *Experimental Mechanics*, 53, pp. 1607–1619. doi: 10.1007/s11340-013-9769-7.

Feldman, D. P. (2012) *Chaos and fractals: an elementary introduction*. Oxford: Oxford University Press.

Foroutan-pour, K., Dutilleul, P. and Smith, D. L. (1999) 'Advances in the implementation of the box-counting method of fractal dimension estimation', *Applied Mathematics and Computation*, 105(2), pp. 195–210. doi: https://doi.org/10.1016/S0096-3003(98)10096-6.

Galarreta, J. F., Kerle, N. and Gerke, M. (2015) 'UAV-based urban structural damage assessment using object-based image analysis and semantic reasoning', *Natural Hazards and Earth System Sciences*, pp. 1087–1101. doi: 10.5194/nhess-15-1087-2015.

Grünthal, G. (1998) 'European macroseismic scale 1998', *Cahiers du centre Européen de Géodynamique et de Séismologie*, 15, pp. 1–99.

Harrar, K. and Hamami, L. (2009) 'Implementation of the box-counting method in radiographic images', in Mastorakis, N. and Sakellaris, J. (eds) *Advances in Numerical Methods*. Boston, MA: Springer US, pp. 299–311. doi: 10.1007/978-0-387-76483-2_26.

Di Ieva, A. (2016) *The Fractal Geometry of the Brain*. Springer.

Di Ieva, A., Grizzi, F., Ceva-Grimaldi, G., Russo, C., Gaetani, P., Aimar, E., Levi, D., Pisano, P., Tancioni, F., Nicola, G., Tschabitscher, M., Dioguardi, N. and Baena, R. R. y (2007) 'Fractal dimension as a quantitator of the microvasculature of normal and adenomatous pituitary tissue', *Journal of Anatomy*. Blackwell Publishing Ltd, 211(5), pp. 673–680. doi: 10.1111/j.1469-7580.2007.00804.x.

Issa, M. A., Issa, M. A., Islam, M. S. and Chudnovsky, A. (2003) 'Fractal dimension—a measure of fracture roughness and toughness of concrete', *Engineering Fracture Mechanics*, 70(1), pp. 125–137. doi: https://doi.org/10.1016/S0013-7944(02)00019-X.

Karperien, A. (2007) 'FracLac for ImageJ-FracLac Advanced User's Manual', *Charles Sturt University, Australia*.
Lopes, R. and Betrouni, N. (2009) 'Fractal and multifractal analysis: A review', *Medical Image Analysis*, 13(4), pp. 634–649. doi: https://doi.org/10.1016/j.media.2009.05.003.

Mandelbrot, B. B. (1983) *The fractal geometry of nature*, *American Journal of Physics*. doi: 10.1017/CBO9781107415324.004.

de Melo, R. H. C. and Conci, A. (2013) 'How Succolarity could be used as another fractal measure in image analysis', *Telecommunication Systems*, 52(3), pp. 1643–1655. doi: 10.1007/s11235-011-9657-3.

Ostwald, M. J. (2013) 'The Fractal Analysis of Architecture: Calibrating the Box-Counting Method Using Scaling Coefficient and Grid Disposition Variables', *Environment and Planning B: Planning and Design*. SAGE Publications Ltd STM, 40(4), pp. 644–663. doi: 10.1068/b38124.

Peitgen, H.-O., Jürgens, H. and Saupe, D. (2006) *Chaos and fractals: new frontiers of science*. New York, NY, USA: Springer Science & Business Media.

Petry, S. and Beyer, K. (2015) 'Cyclic test data of six unreinforced masonry walls with different boundary conditions', *Earthquake Spectra*. Earthquake Engineering Research Institute, 31(4), p. 2459–2484. doi: 10.1193/101513EQS269.

Plotnick, R. E., Gardner, R. H. and O'Neill, R. V (1993) 'Lacunarity indices as measures of landscape texture', *Landscape Ecology*, 8(3), pp. 201–211. doi: 10.1007/BF00125351.

Roy, A., Perfect, E., Dunne, W. M. and McKay, L. D. (2007) 'Fractal characterization of fracture networks: An improved box-counting technique', *Journal of Geophysical Research: Solid Earth*, 112(B12), p. n/a-n/a. doi: 10.1029/2006JB004582.

Sandau, K. (1996) 'A note on fractal sets and the measurement of fractal dimension', *Physica A: Statistical Mechanics and its Applications*, 233(1), pp. 1–18. doi: https://doi.org/10.1016/S0378-4371(96)00248-8.

Sandau, K. and Kurz, H. (1997) 'Measuring fractal dimension and complexity — an alternative approach with an application', *Journal of Microscopy*. Blackwell Science Ltd, 186(2), pp. 164–176. doi: 10.1046/j.1365-2818.1997.1270685.x.

So, G.-B., So, H.-R. and Jin, G.-G. (2017) 'Enhancement of the Box-Counting Algorithm for fractal dimension estimation', *Pattern Recognition Letters*, 98(Supplement C), pp. 53–58. doi: https://doi.org/10.1016/j.patrec.2017.08.022.

Sun, H. Q., Ding, J., Guo, J. and Fu, D. L. (2011) 'Fractal research on cracks of reinforced concrete beams with different aggregates sizes', in *Advanced Materials Research*. Trans Tech Publ, pp. 1818–1822.

Yang, W., He, X. and Dai, L. (2017) 'Damage behaviour of concrete beams reinforced with GFRP bars', *Composite Structures*, 161(Supplement C), pp. 173–186. doi: https://doi.org/10.1016/j.compstruct.2016.11.041.